Accuracy measurements and improvement for complete characterization of optical pulses from nonlinear processes via multiple spectral-shearing interferometry

Adam S. Wyatt,[1,*] **Alexander Grün,**[2] **Philip K. Bates,**[2]
Olivier Chalus,[2,4] **Jens Biegert,**[2,3] **and Ian A. Walmsley**[1]

[1]*Clarendon Laboratory, University of Oxford, Parks Road, Oxford, OX1 3PU, UK*
[2]*ICFO — Insitut de Ciencies Fotoniques, Mediterranean Technology Park, 08860 Castelldefels, Barcelona, Spain*
[3]*ICREA — Institucio Catalana de Recerca i Estudis Avanc ats, 08010 Barcelona, Spain*
[4]*Currently at Thales Optronique S.A., DSL, 78995 Elancourt Cedex, France*
**a.wyatt1@physics.ox.ac.uk*

http://ultrafast.physics.ox.ac.uk

Abstract: We demonstrate that multiple spectral-shearing interferometry increases the precision and accuracy of measurements of the spectral phase of a complex pulse (time-bandwidth product = 125) arising from self-phase modulation in a gas filled capillary. We verify that the measured interferometric phase is accurate to 0.1 rad across the full bandwidth by checking the consistency between the spectral phases of each individual shear measurement. The accuracy of extracting pulse parameters (group delay dispersion, pulse duration and peak intensity) for single shear measurements were verified to better than 10% by comparison with the multishear reconstruction. High order space-time coupling is quantified across a single transverse dimension, verifying the suitability of such pulses for use in strong field experiments.

OCIS codes: (320.0320) Ultrafast optics; (320.7100) Ultrafast measurements; (320.5520) Pulse compression; (190.1900) Diagnostic applications of nonlinear optics; (190.7110) Ultrafast nonlinear optics.

References and links

1. D. R. Austin, T. Witting, and I. A. Walmsley, "High precision self-referenced phase retrieval of complex pulses with multiple-shearing spectral interferometry," J. Opt. Soc. Am. B **26**, 1818–1830 (2009).
2. D. R. Austin, T. Witting, and I. A. Walmsley, "Resolution of the relative phase ambiguity in spectral shearing interferometry of ultrashort pulses," Opt. Lett. **35**, 1971–1973 (2010).
3. I. A. Walmsley and C. Dorrer, "Characterization of ultrashort electromagnetic pulses," Adv. Opt. Photon. **1**, 308–437 (2009).
4. R. Trebino, *Frequency-Resolved Optical Gating: The Measurement of Ultrashort Laser Pulses* (Springer, 2002).
5. R. Trebino, K. W. DeLong, D. N. Fittinghoff, J. N. Sweetser, M. A. Krumbügel, B. A. Richman, and D. J. Kane, "Measuring ultrashort laser pulses in the time-frequency domain using frequency-resolved optical gating," Rev. Sci. Instrum. **68**, 3277–3295 (1997).

#156765 - $15.00 USD Received 19 Oct 2011; revised 13 Nov 2011; accepted 14 Nov 2011; published 28 Nov 2011

6. C. Iaconis and I. A. Walmsley, "Spectral phase interferometry for direct electric-field reconstruction of ultrashort optical pulses," Opt. Lett. **23**, 792–794 (1998).
7. C. Iaconis and I. A. Walmsley, "Self-referencing spectral interferometry for measuring ultrashort optical pulses," IEEE J. Quantum Electron. **35**, 501–509 (1999).
8. R. H. Stolen and C. Lin, "Self-phase-modulation in silica optical fibers," Phys. Rev. A **17**, 1448–1453 (1978).
9. D. W. Schumacher, F. Weihe, H. G. Muller, and P. H. Bucksbaum, "Phase dependence of intense field ionization: A study using two colors," Phys. Rev. Lett. **73**, 1344–1347 (1994).
10. B. Schenkel, J. Biegert, U. Keller, C. Vozzi, M. Nisoli, G. Sansone, S. Stagira, S. De Silvestri, and O. Svelto, "Generation of 3.8-fs pulses from adaptive compression of a cascaded hollow fiber supercontinuum," Opt. Lett. **28**, 1987–1989 (2003).
11. T. Brabec and F. Krausz, "Intense few-cycle laser fields: Frontiers of nonlinear optics," Rev. Mod. Phys. **72**, 545–591 (2000).
12. F. X. Kärtner, *Few-Cycle Laser Pulse Generation and Its Applications* (Springer, 2004).
13. J. M. Dudley and J. R. Taylor, "Ten years of nonlinear optics in photonic crystal fiber," Nat. Photonics **3**, 85–90 (2009).
14. J. Kasparian, M. Rodriguez, G. Méjean, J. Yu, E. Salmon, H. Wille, R. Bourayou, S. Frey, Y.-B. André, A. Mysyrowicz, R. Sauerbrey, J.-P. Wolf, and L. Wöste, "White-light filaments for atmospheric analysis," Science **301**, 61–64 (2003).
15. W. Kornelis, J. Biegert, J. W. G. Tisch, M. Nisoli, G. Sansone, C. Vozzi, S. De Silvestri, and U. Keller, "Single-shot kilohertz characterization of ultrashort pulses by spectral phase interferometry for direct electric-field reconstruction," Opt. Lett. **28**, 281–283 (2003).
16. W. Kornelis, M. Bruck, F. W. Helbing, C. P. Hauri, A. Heinrich, J. Biegert, and U. Keller, "Single-shot dynamics of pulses from a gas-filled hollow fiber," Appl. Phys. B: Lasers Opt. **79**, 1033–1039 (2004).
17. D. R. Solli, C. Ropers, P. Koonath, and B. Jalali, "Optical rogue waves," Nature (London) **450**, 1054–1057 (2007).
18. L. Gallmann, G. Steinmeyer, D. H. Sutter, T. Rupp, C. Iaconis, I. A. Walmsley and U. Keller, "Spatially resolved amplitude and phase characterization of femtosecond optical pulses," Opt. Lett. **26** 26, 96–98 (2001).
19. C. Dorrer and I. A. Walmsley, "Simple linear technique for the measurement of space-time coupling in ultrashort optical pulses," Opt. Lett. **27**, 1947–1949 (2002).
20. C. Dorrer and I. A. Walmsley, "Precision and consistency criteria in spectral phase interferometry for direct electric-field reconstruction," J. Opt. Soc. Am. B **19**, 1030–1038 (2002).
21. M. Takeda, H. Ina, and S. Kobayashi, "Fourier-transform method of fringe-pattern analysis for computer-based topography and interferometry," J. Opt. Soc. Am. **72**, 156–160 (1982).
22. A. S. Wyatt, I. A. Walmsley, G. Stibenz, and G. Steinmeyer, "Sub-10 fs pulse characterization using spatially encoded arrangement for spectral phase interferometry for direct electric field reconstruction," Opt. Lett. **31**, 1914–1916 (2006).
23. C. Dorrer, P. Londero, and I. A. Walmsley, "Homodyne detection in spectral phase interferometry for direct electric-field reconstruction," Opt. Lett. **26**, 1510–1512 (2001).
24. J. R. Birge and F. X. Kärtner, "Analysis and mitigation of systematic errors in spectral shearing interferometry of pulses approaching the single-cycle limit," J. Opt. Soc. Am. B **25**, A111–A119 (2008).
25. A. S. Wyatt, Clarendon Laboratory, University of Oxford, Parks Road, Oxford, OX1 3PU, UK, is preparing a manuscript to be called "Generalized multishearing interferometry."
26. C. Dorrer and I. A. Walmsley, "Accuracy criterion for ultrashort pulse characterization techniques: application to spectral phase interferometry for direct electric field reconstruction," J. Opt. Soc. Am. B **19**, 1019–1029 (2002).
27. A. S. Wyatt and I. A. Walmsley, "Analysis of space-time coupling in sea-spider measurements," in *Lasers and Electro-Optics 2009 and the European Quantum Electronics Conference. CLEO Europe - EQEC 2009. European Conference on*, Germany, 14–15 June 2009.
28. P. Gabolde and R. Trebino, "Single-shot measurement of the full spatio-temporal field of ultrashort pulses with multi-spectral digital holography," Opt. Express **14**, 11460–11467 (2006).
29. P. Bowlan, P. Gabolde and R. Trebino, "Directly measuring the spatio-temporal electric field of focusing ultrashort pulses," Opt. Express **15**, 10219–10230 (2007).
30. C. Dorrer, E. M. Kosik, and I. A. Walmsley, "Spatio-temporal characterization of the electric field of ultrashort optical pulses using two-dimensional shearing interferometry," Appl. Phys. B: Lasers Opt. **74**, S209–S217 (2002).
31. B. Alonso, I. J. Sola, Ö. Varela, J. Hernández-Toro, C. Méndez, J. S. Román, A. Zaïr and L. Roso, "Spatiotemporal amplitude-and-phase reconstruction by Fourier-transform of interference spectra of high-complex-beams," J. Opt. Soc. Am. B **27**, 933–940 (2010).

#156765 - $15.00 USD Received 19 Oct 2011; revised 13 Nov 2011; accepted 14 Nov 2011; published 28 Nov 2011

1. Introduction

Ultrashort optical pulses provide a means both to study and to control dynamics of atoms, molecules and solids on time-scales comparable with electronic and nuclear motion. These capabilities are predicated on the ability to shape the space-time fields incident on the matter, and to measure the scattered or radiated fields with high accuracy and precision. New insight into and control of these dynamical processes will therefore accrue from better ways to shape and to measure broadband coherent optical fields across a range of wavelengths and timescales.

In recent publications it was shown that spectral multishearing interferometry can be used to increase the precision of the measurement whilst still maintaining spectral resolution and to overcome any relative phase ambiguities between disjoint spectral regions [1, 2]. In this paper we demonstrate a means to quantify and improve the accuracy and precision for complete characterization of ultra-broadband optical pulses generated via a nonlinear process (self-phase modulation in a gas-filled capillary) by the application of spectral multishearing interferometry to the measurement of the spectral phase of the pulse. Precision is enhanced compared to single-shearing interferometry due to an over-determination of the spectral phase; accuracy is enhanced by ensuring the relative phase across spectral nulls are recovered. The accuracy in the reconstruction of the spectral phase is estimated by comparing the different shear measurements. We use this method of experimentally estimating the accuracy of the spectral phase reconstruction to perform an extensive systematic study on the quality of the space-time characterization of a hollow-core fiber pulse compressor system for generating intense few-cycle pulses for use in strong field experiments. We utilize the improved accuracy to measure the complete temporal pulse as a function of a single transverse dimension and to quantify the complexity of the pulse based on its time-bandwidth product.

1.1. Choice of a measurement technique

Currently there exists a plethora of devices for complete temporal characterization of ultrafast optical pulses [3]; the most commonly used devices are based on spectrographic or spectral-shearing methods (e.g. FROG [4, 5] and SPIDER [6, 7]). Each specific device has its own advantages and disadvantages and variants of these methods have been designed for measuring a particular class or set of classes of pulses. One particular set of pulses of current interest are those that have been modified by a nonlinear process, such as self-phase modulation [8] or ionization [9]. These processes have proven useful for generating intense few-cycle pulses [10] for use in strong-field physics [11, 12], super-continuum generation [13] for spectroscopy and self-guided propagation for LIDAR [14], to name a few examples. Since the electric field is a fundamental entity in these processes, and is the quantity studied in simulations, and since the dynamics of the nonlinear propagation can be very sensitive to the incident (space-time) field, quantitative agreement between experiments and simulations can only be obtained if accurate and precise (space-time) measurements of the electric field incident on and emerging from the nonlinear processes are made. In the case of highly nonlinear processes such as filamentation, the accuracy requirements for these measurements are much more stringent if one is to be able to unambiguously determine the relative contributions of different nonlinear processes (e.g. high-order Kerr effects and ionization). Additionally, single-shot acquisition may also be important to understand shot-to-shot statistics [15, 16], for example in studying optical rogue waves [17]. Hence improving the accuracy, precision and capabilities of complete characterization methods are still vitally important in the study of nonlinear dynamics.

Complete characterization of pulses from nonlinear interactions is a challenging task: (1) the generation of new frequencies prevent reference based methods from being used without a well characterized external source with the same bandwidth; (2) fragmentation into multiple pulses and disjoint spectral regions increase the complexity of the pulse under study and therefore

#156765 - $15.00 USD Received 19 Oct 2011; revised 13 Nov 2011; accepted 14 Nov 2011; published 28 Nov 2011

increase the spectral and temporal resolution requirements; (3) coupling between the spatial and spectral/temporal degrees of freedom require a device that is capable of measuring this space-time coupling, (4) the nonlinear interaction is more sensitive to perturbations in the input field, hence single-shot acquisition is preferred.

Interferometric methods have several advantages over spectrographic and tomographic methods in respect to measuring pulses from nonlinear interactions: the measured data and information extracted are encoded with the same number of dimensions (e.g. an imaging spectrometer can be used to measure the spectral and one spatial dimension of a pulse on a two-dimensional array detector in a single acquisition), and thus can easily be extended to measure space-time coupling in the pulse [18, 19]. The measured spectrum is linear in the input spectral intensity, enabling the measurement of low intensity spectral regions. Additionally, low intensity temporal sub-pulses manifest themselves as a strong modulation in the spectral intensity and/or oscillations in the spectral phase and so can often be easily detected. Finally, the reconstruction of the spectral phase is algebraic (non-iterative), providing a means to test the precision and consistency of the data; and local, thus any error in the spectral phase can be attributed to a specific spectral region.

The most common interferometric self-referencing methods are based on spectral-shearing interferometry, which has some disadvantages. For example, the measured interferometric phase is integrated across the spectrum to obtain the test pulse spectral phase. In the case of a nonlinear process, the output pulses have a strongly modulated spectrum that needs to be sampled with high spectral resolution; but as the bandwidth can span an octave or more, this can result in the accumulation of a large error across the full spectrum. Additionally, the relative phase of disjoint spectral regions (i.e. spectral regions separated by a region of zero or low spectral intensity) can be lost since the measured phase in the spectral null is undefined. Finally, these methods contain no direct temporal information and so at first would appear to have no means to check the integrity and thus accuracy of the reconstructed temporal profile. Consistency checks on single shear measurements [20] ensure a suitable shear is used for the pulse being measured, but cannot verify other systematic errors, for example ensuring the ancillary pulses are monochromatic over the test-pulse duration. By performing spectral multishearing interferometry, these limitations can be overcome and additional consistency and accuracy tests can be performed, whilst maintaining all the advantages of interferometry previously described.

2. Experimental setup

The spectral phase of the test pulse (TP) is measured by means of spectral-shearing interferometry: two spectrally shifted pulse replicas are interfered and the spectral phase extracted from the interferogram (referred to later as the SPIDER phase) is extracted via the Takeda algorithm [21]. For small spectral shears, this phase is approximately equal to the spectral phase gradient, or chirp of the TP. Although this provides for an intuitive understanding, the phase of the TP can be recovered exactly (in the absence of noise) via concatenation with a sampling frequency equal to the spectral shear. In the case of multishearing interferometry, the purpose is to find the spectral phase that is most consistent with measurements made with various shears. This can be achieved via a simple matrix inversion adapted from [1].

For our measurements, we utilize a spatially encoded arrangement spectral phase interferometry for direct electric-field reconstruction (SEA-SPIDER) device specifically designed for the measurement of few-cycle pulses. The details for this device can be found in [22]; for clarity the concept is explained in Fig. 1. The spectral shear is varied by altering the arrival time of one of the chirped pulses with respect to the other. A calibration trace is taken by setting the delay between the two chirped pulses to zero, such that the spectral shear is then zero. Since all measurements are referenced to this calibration trace, the measurements presented here cor-

#156765 - $15.00 USD Received 19 Oct 2011; revised 13 Nov 2011; accepted 14 Nov 2011; published 28 Nov 2011

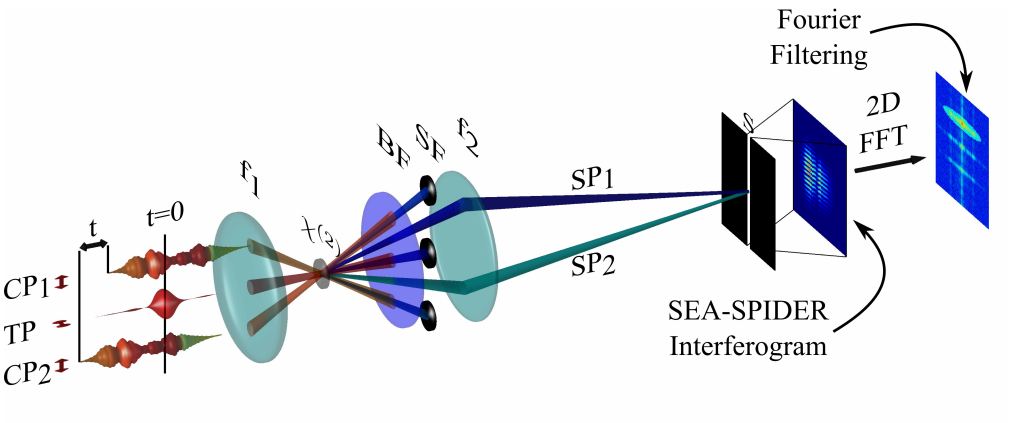

Fig. 1. SEA-SPIDER concept. The two signal pulses (SP_1 & SP_2) are created via type II sum frequency generation (SFG) in a $\chi^{(2)}$ nonlinear crystal (e.g. 30 μm BBO) of the test pulse (TP) with two spatially tilted and highly chirped ancillary pulses (CP_1 & CP_2) separated in time by a delay τ. During the SFG, the TP interacts with two different quasi-monochromatic frequencies, resulting in two spectrally sheared replicas of the test pulse centered near twice the fundamental frequency. The upconverted interference pattern is filtered using a blue filter (BF) and spatial filter (SF), then imaged onto the entrance slit of an imaging spectrometer. The spatial tilt results in spatial fringes, enabling the extraction of the spatially-dependent spectral phase. Experimentally, focusing mirrors are used for f_1 and f_2 to prevent chromatic aberration and dispersion of the TP.

respond to HOT-SPIDER [23] where one of the signal pulses (SP_2) acts as a local oscillator and thus its spectral phase is irrelevant. A major advantage of this geometry is that there is no error in the reconstructed phase due to an error in the calibration of the time-delay between the pulses [24]: this is guaranteed to be zero since the pulse is referenced to itself. We chose a scanning method to enable measurements on the space-time coupling of the pulses emerging from the hollow-core fiber compressor, to ensure that they were suitable for strong field experiments such as high harmonic generation. One can perform the exact same analysis presented in this paper on single-shot measurements made with the device described in [2] if shot-to-shot statistics are required.

Since the different spectral shear measurements are taken sequentially by varying the delay, τ, between the two chirped pulses via a manual translation stage, it is necessary to ensure that the pulse being measured does not vary significantly during the experiment. Therefore we measured the fundamental spectrum on a fiber-coupled spectrometer between each successive shear measurement. The measured spectrum and its statistics are shown in Fig. 2. The intensity error in Fig. 2 (a) is calculated as a percentage error with respect to the ensemble average without normalization of each individual measurement. We do not normalize to a constant energy to emphasize the shot-to-shot stability. Since the total nonlinearity after propagating through the capillary is significant (resulting in spectral broadening by a factor of three or more), any fluctuations in the pulse shape (as a result of intensity, phase or coupling instabilities) would also manifest themselves in the broadened spectrum. Using a motorized stage would enable automation of the process, significantly reducing the acquisition time and thus minimizing the effects of fluctuations in the TP.

#156765 - $15.00 USD Received 19 Oct 2011; revised 13 Nov 2011; accepted 14 Nov 2011; published 28 Nov 2011

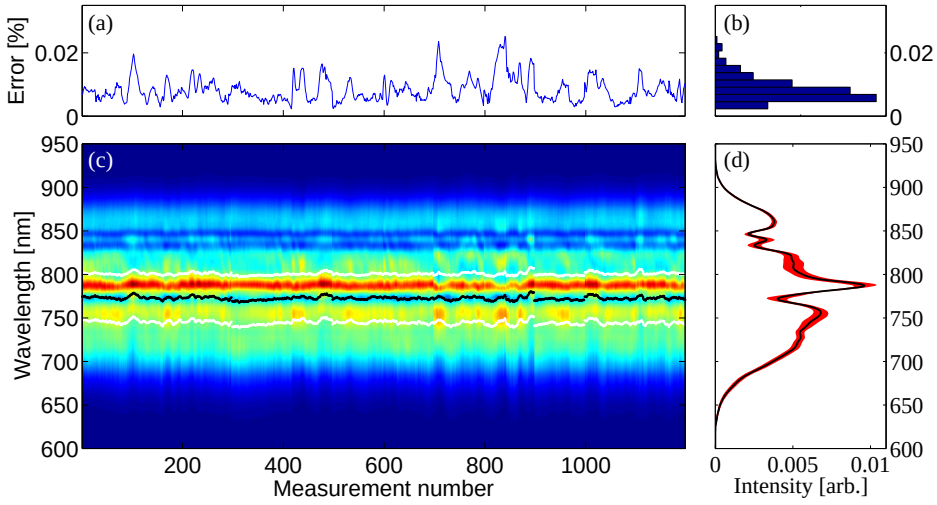

Fig. 2. Pulse spectrum variation during measurement acquisition. (a) Intensity error between measured spectrum and ensemble average. (b) Histogram of spectral error (counts along horizontal axis). (c) Measured spectra (blue=zero intensity, red=maximum intensity, smoothed to remove electronic read-out noise); the pulse's spectral moment (black dots) and RMS width (white dots) are superimposed. (d) Ensemble average (black line) and standard deviation (red band).

3. Spectral phase reconstruction

After performing Fourier filtering of the measured SPIDER interferogram via the Takeda algorithm, the interferometric term $D(\omega,\Omega) = E_{\mathrm{TP}}(\omega-\omega_{\mathrm{CP}}-\Omega)E^{*}_{\mathrm{TP}}(\omega-\omega_{\mathrm{CP}})$ is obtained in terms of the test pulse analytic field E_{TP}. Here, ω_{CP} is the quasi-CW upconversion frequency derived from CP_1 during the calibration measurement and Ω is the spectral shear (defined such that a positive shear shifts the pulse to higher frequencies). The SPIDER phase is then defined as

$$\begin{aligned}\theta(\omega,\Omega) &= \arg\left[D(\omega+\omega_{\mathrm{CP}},\Omega)D^{*}_{\mathrm{cal}}(\omega+\omega_{\mathrm{CP}})\right] \\ &= \phi_{\mathrm{TP}}(\omega-\Omega)-\phi_{\mathrm{TP}}(\omega).\end{aligned} \tag{1}$$

This equation can be expressed in terms of a matrix equation relating measured SPIDER phases to the unknown test pulse phase via a set of linear operations:

$$\theta_{(m+Ms)} = \sum_{n=0}^{N-1}\left[A_{(m+Ms)n}-B_{(m+Ms)n}\right]\phi_n, \tag{2}$$

where $\phi_n = \phi(\omega_n)$ is the desired test pulse phase sampled at points $\{\omega_n\}$ and $\theta_{(m+Ms)} = \theta(\omega_m,\Omega_s)$ is the measured two-dimensional SPIDER phase mapped into a vector and sampled at frequencies $\{\omega_m\}$ for shears $\{\Omega_s\}$; $n = 0,1,\ldots,N-1$, $m = 0,1,\ldots,M-1$, and $s = 0,1,\ldots,S-1$ are integer indices; N is the number of sampling points for the reconstructed test pulse phase; M is the number of frequency sampling points for the measured SPIDER phase and S is the number of shear measurements.

If $\omega_m = \omega_n = \omega_0 + n\Omega_0$ and $\Omega_s = a_s\Omega_0$ where a_s is an integer (ω_0 is the first sampled frequency and $a_0 = 1$), then $A_{(m+Ms)m} = -B_{(m+Ms)(m+a_s)} = 1$ and zero at all other points, as

#156765 - $15.00 USD Received 19 Oct 2011; revised 13 Nov 2011; accepted 14 Nov 2011; published 28 Nov 2011

described in [1]. Since this requires the shears to be integer multiples of each other, it is necessary to be able to accurately set the shear during acquisition, or to be able to oversample the two-dimensional SPIDER phase and then interpolate onto the evenly sampled grid. The former method is not always practical or feasible, whereas the latter method requires the shear axis to be sampled with the same resolution as the spectral axis; the resolution being determined by the test pulse shape according to the sampling theorem. In this situation, only a subset of the measured data is directly used in the reconstruction; maximal accuracy and precision can only be achieved (for a given amount of resources) if the whole data set is used directly. Therefore we proceed with a slightly more general approach: the test pulse phase at frequencies $\{\omega_m\}$ — the measured sampling points — and $\{\omega_m - \Omega_s\}$ are calculated via a piece-wise polynomial interpolation of the evenly sampled unknown test pulse phase sampled at frequencies $\{\omega_n\}$. The details of this method are described in [25]. The resulting matrix is now a vertical concatenation of band-diagonal (c.f. bi-diagonal) sub-matrices, with the width of the band determined by the order of the interpolation. We find that cubic interpolation is normally optimal.

4. Results

For each value of the shear, 100 SEA-SPIDER interferograms were recorded to enable statistics to be performed on the reconstructed data and any parameters extracted from this data; the SPIDER phase was extracted from each interferogram using a 2D Takeda algorithm and then only the spectral information at the center of the beam was used for the analysis below. When performing the temporal reconstruction, we used the mean spectral intensity with high frequency noise (due to electronic readout noise) removed. Since we used a silver focusing mirror to image the crystal onto the spectrometer, the detection of wavelengths below 400 nm are compromised. We therefore also spectrally filtered the fundamental spectrum for use in determining the accuracy and temporal intensity (indicated by the yellow region in Fig. 3(a)). In any real experiment, fluctuations in the spectral intensity would also change the temporal reconstruction. However, the purpose of this paper is to demonstrate the effect different sized shears have on the spectral phase reconstruction and to demonstrate the improvements obtained by using the multishear algorithm. Hence we want to isolate the effects of inaccuracies and imprecision in the spectral phase from fluctuations/inaccuracies in the spectral intensity. The dominant effect causing dispersion in the test pulse temporal reconstructions arise from the test pulse spectral phase reconstruction and not from the spectral intensity.

4.1. Accuracy measurements

One important feature of performing multiple shears is that this provides multiple independent measurements of the same pulse. Therefore each shear measurement should reconstruct the same spectral phase. This is illustrated in Fig. 3(a), which plots the reconstructed TP spectral phase for the different shear measurements via the mid-point/trapezium integration method [26], the multishear reconstruction, the TP spectral intensity and the signal pulse spectral intensity for $\Omega = 0$ (shifted by ω_{CP} to overlap with the fundamental). The 100 measurements for each phase reconstruction enables the probability density function for $\phi_{\mathrm{TP}}(\omega)$ to be estimated; this is indicated by the intensity of the lines. The agreement of the global phase (e.g. the GDD) between the different reconstructions is excellent. Note that in the case of a large spectral shear, the phase in the wings should be disregarded since the intensity of the interferogram in this region is very low. Two important features can be seen as the magnitude of the shear is increased: (1) the precision improves (the deviation from the mean of the individual measurements at a given shear is reduced) and (2) the fine structure on the phase is washed out. The multishear reconstruction remains precise and recovers the fine structure simultaneously, thus qualitatively showing an improvement in precision and accuracy compared to single-shear

#156765 - $15.00 USD Received 19 Oct 2011; revised 13 Nov 2011; accepted 14 Nov 2011; published 28 Nov 2011

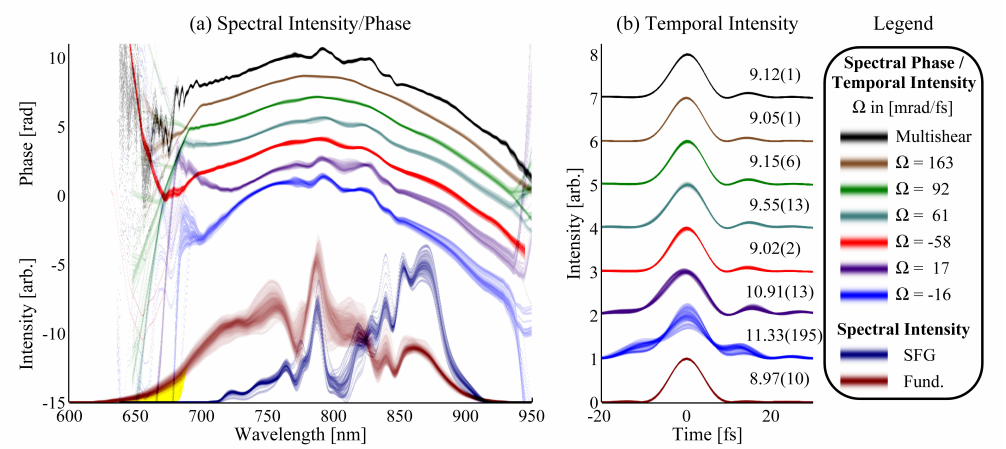

Fig. 3. Spectral and temporal reconstructions; the probability that the phase/intensity is a given value is represented by the intensity of the line at that value. (a) Spectral intensity and phase. The phases have been offset from each other for clarity. The SP spectrum has been shifted in wavelength to overlap with the fundamental. (b) Temporal intensity reconstructions and FWHM pulse durations after phase compensation — see text; the color scheme is the same as in (a). The Fourier transform limited temporal profile (dark red) is calculated from the fundamental spectrum.

measurements.

The consistency of the different shear measurements can be calculated by using the spectral phase reconstructed via the multishear algorithm to estimate the SPIDER phase for each individual shear measurement (Fig. 4). For each shear, the probability density function is indicated by the intensity of the line, and the SPIDER phase estimated from the multishear spectral phase is superimposed as a black dotted line. The agreement is excellent for all shears where the interferometric amplitude (not drawn for clarity) is above the noise floor. It is clear that the fine structure on the SPIDER phase is physical since it is reproduced for all shears. Therefore we can conclude that all measurements are consistent with each other and thus we can believe that the reconstructed spectral phase is an accurate estimate of the true spectral phase.

We quantify the accuracy estimate of the measurement by calculating the RMS phase error [26], $\eta(\Omega)$, between the measured SPIDER phase, $\theta_{\text{meas}}(\omega,\Omega)$ and the SPIDER phase calculated from the test-pulse phase reconstructed from the multishear algorithm, $\theta_{\text{ms}}(\omega,\Omega)$, as follows

$$\eta(\Omega) = \left\{ \frac{\int |D(\omega,\Omega)|^2 \left[\theta_{\text{ms}}(\omega,\Omega) - \theta_{\text{meas}}(\omega,\Omega)\right]^2 \mathrm{d}\omega}{\int |D(\omega,\Omega)|^2 \mathrm{d}\omega} \right\}^{1/2}. \tag{3}$$

The RMS phase error is measured to be approximately 0.1 rad in all cases, quantifying excellent agreement. In the spectral range 420–440 nm, the precision in the SPIDER phase is reduced (especially near 420 nm) as a result of the nulls in the spectral intensity. This is the main cause of poor precision in the reconstructed spectral phase for small shears since the accumulation of phase error resulting from the integration / concatenation across this spectral region is quite large. Larger shears require less points in the concatenation and therefore the accumulated phase error is smaller, resulting in higher precision. In the multishear algorithm, over-determination of the measured phase reduces the effect of random errors.

#156765 - $15.00 USD Received 19 Oct 2011; revised 13 Nov 2011; accepted 14 Nov 2011; published 28 Nov 2011

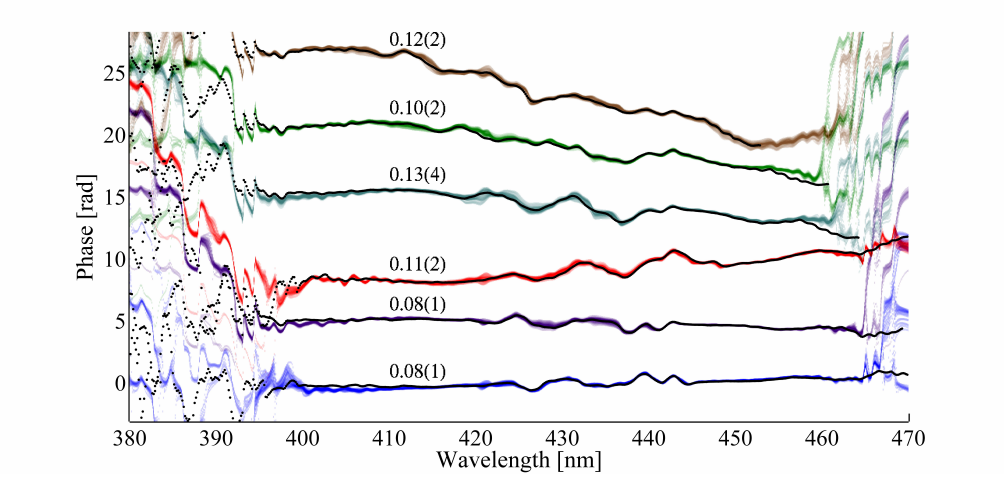

Fig. 4. Extracted SPIDER phases for the different shear measurements. The intensity of each line represents the probability distribution calculated from 100 measurements for each individual shear. For each shear, the SPIDER phase has also been calculated using the TP spectral phase reconstructed via the multishear algorithm and is superimposed as a black dotted line. The RMS phase error between the measured and reconstructed SPIDER phase for each shear is written above each measurement. The SPIDER phases have been offset from each other for clarity.

Figure 3(b) plots the temporal reconstruction of the test-pulse after compensating the spectral phase accumulated after propagating to the center of a vacuum chamber for high harmonic generation experiments (1 mm fused silica entrance window and 1.6 m of additional path length in air). The pulse duration measured at full width half maximum (FWHM) is shown next to each plot. Again the agreement between the the different shear measurements is excellent, except for the two shears of the smallest magnitude. This is a result of poor precision in regions of low spectral intensity, thus increasing the error in the relative spectral phase of adjacent spectral regions separated by a spectral null.

Table 1 lists a selection of quantities that can be extracted from the reconstructed data (GDD, pulse duration and peak power), as well as the precision and accuracy of the reconstructed data. This data quantitatively demonstrates the features described above, namely that the precision improves as the magnitude of the shear is increased. The accuracy however remains acceptable (0.1–0.2), but not optimal (< 0.1) for all but the smallest shears. This can be attributed to the fact that the size of the shear is a balance between a large enough shear to span spectral nulls such that the relative phase between these two regions is well defined, and a small enough shear to accurately recover the fine structure. From this data, it is clear that in this case a spectral shear of approximately 10% of the pulse bandwidth is optimal; this value is specific to this pulse shape. If a finer spectral resolution was required, a smaller shear would be necessary, resulting in poorer accuracy in the reconstruction.

4.2. Pulse complexity

As discussed in §1.1, nonlinear propagation can result in quite complex optical pulses, even in the case of generation of few-cycle pulse via nonlinear pulse compression. The complexity of a pulse can be quantified by its time-bandwidth product (TBP). One such definition of TBP is the number of points required to sufficiently sample its analytic function, i.e. the ratio of the pulse

#156765 - $15.00 USD Received 19 Oct 2011; revised 13 Nov 2011; accepted 14 Nov 2011; published 28 Nov 2011

Table 1. Quantitative results from multishear, concatenation (top line for each shear) and integration (bottom line for each shear) methods. Three quantities of interest have been chosen: (1) the GDD ($\phi^{(2)}$, calculated via a weighted polynomial fit about the center of mass of the fundamental spectrum) of the pulse before compensating the optical path to the experiment , (2) the pulse duration measured at FWHM (Δt_{FWHM}) and (3) the peak power (I_0) of the pulse after compensating the optical path to the experiment. In each case, the mean values from the sample distributions are shown along with the standard deviation of the sample estimate in brackets, and hence the precision of the estimated value (note this is not the standard error in the estimate of the mean). The percentage error (Δ) has been calculated with respect to the multishear value, since this is deemed as the best estimate of the true value from our experimental data. The precision (σ) is a measure of the standard deviation of the RMS pulse error for the sample distribution [20]. The accuracy (ε) is calculated from the RMS error between the pulse means reconstructed from the multishear algorithm and the individual shear reconstructions [26].

Shear	$\phi^{(2)}$		Δt_{FWHM}		P_0		σ	ε
[rad/fs]	[fs^2/rad]	Δ [%]	[fs]	Δ [%]	[TW]	Δ [%]		
Multi	-41.9 (0.4)		9.12 (0.01)		45.2 (0.2)		0.03	
163.3 (5.2)	-35.9 (2.0)	-14.29	9.14 (0.00)	0.2	51.3 (0.1)	13.3	0.05	0.07
	-40.5 (0.9)	-3.29	9.05 (0.01)	-0.8	49.0 (0.3)	8.4	0.03	0.24
92.4 (0.3)	-46.5 (1.4)	10.85	9.11 (0.05)	-0.2	40.5 (0.7)	-10.5	0.05	0.12
	-41.1 (1.0)	-1.90	9.16 (0.06)	0.4	46.1 (0.5)	2.0	0.04	0.17
61.3 (0.5)	-40.0 (2.0)	-4.54	9.48 (0.16)	3.9	40.9 (1.5)	-9.6	0.07	0.18
	-38.4 (1.7)	-8.26	9.56 (0.13)	4.8	42.4 (0.7)	-6.3	0.06	0.21
-58.3 (5.0)	-45.4 (1.8)	8.30	8.86 (0.03)	-2.8	47.4 (0.9)	4.7	0.07	0.16
	-42.7 (1.7)	1.77	9.02 (0.02)	-1.1	48.0 (0.9)	6.1	0.05	0.15
17.3 (1.8)	-40.7 (2.8)	-2.88	10.37 (0.13)	13.7	34.9 (1.1)	-22.9	0.11	0.35
	-39.6 (2.6)	-5.48	10.89 (0.12)	19.4	33.4 (0.9)	-26.3	0.11	0.37
-15.7 (0.2)	-61.5 (4.1)	46.78	13.11 (4.46)	43.7	28.7 (4.2)	-36.5	0.15	0.61
	-58.8 (4.3)	40.21	11.33 (1.94)	24.2	31.3 (4.1)	-30.9	0.16	0.57

spectrum to the sampling rate determined by the sampling theorem:

$$N_{\mathrm{dB}} = \frac{BT}{2\pi}, \tag{4}$$

where B is the full spectral support (in angular frequency) and T the full temporal support for the pulse. Since a pulse cannot have compact temporal and spectral support simultaneously, the dynamic range must be specified in order to determine N, this is denoted in decibels as a subscript. This value depends strongly on the application. For example in high harmonic generation with a peak intensity of $\lesssim 10^{15}\,\mathrm{Wcm}^{-2}$, a dynamic range of 20 dB should suffice. Laser particle acceleration, however, with peak-powers $> 10^{18}\,\mathrm{Wcm}^{-2}$ will require much higher dynamic range since a very weak pre-pulse/background will still have sufficient intensity to field-ionize the medium and thus change the dynamics of the process. It is also necessary to consider numerical aliasing of the analytic signal, e.g. a sub-pulse with peak power $\sim 1\%$ of the main pulse peak power and aliased to coincide with the peak of the main pulse in the time domain can modify the main pulse peak power by up to $\sim 20\%$ as a result of numerical interference of the two fields. Thus it is necessary to ensure the pulse is measured with a dynamic range at least 100

#156765 - $15.00 USD Received 19 Oct 2011; revised 13 Nov 2011; accepted 14 Nov 2011; published 28 Nov 2011

times as required for their application. For example, we would recommend a dynamic range in the measurement of 40–50 dB for high harmonic generation. Performing very high dynamic range measurements is a challenging task. We used the multiple shears to estimate the accuracy of the temporal reconstruction down to 50 dB, thus enabling the quantification of the TBP at this level. The 50 dB TBP was measured to be 125 ($N_{50}^{\mathrm{FTL}} = 45$), indicating the importance of accurate spectral phase measurements.

4.3. Space-time reconstruction

Since SEA-SPIDER spatially resolves the spectral phase, it is possible to perform a space-time reconstruction of the test pulse (in one transverse direction). This requires the fundamental spectrum to be spatially resolved as well. However, there are a couple of effects that need to be considered. The first is that the upconversion process results in the signal pulses having pulse-front tilt since the group front of the signal pulses matches that of the test pulse, but the direction of propagation is off-axis due to conservation of momentum [27]. Therefore an accurate calibration of the upconversion geometry is required to account for this. The second effect is that any space-time coupling on the ancillaries is also mapped to the signal pulses. It is therefore important to spatially filter the ancillaries [27]. In the absence of an accurate calibration of the upconversion geometry, and without sufficient spatial filtering, it is necessary to assume that the relative time-delay of the pulse at each spatial position is unknown. The relative phase information between each spatial position cannot be measured directly with SEA-SPIDER; simply spatially resolving a spectral-shearing interferogram alone is not sufficient — either a reference wavefront or additional operations are required (e.g. sampling a single position, adding an additional lateral shear, measurements at multiple longitudinal positions) [28–31]. Therefore SEA-SPIDER alone is unable to measure the spatial phase, which is required to propagate the pulse to any arbitrary plane.

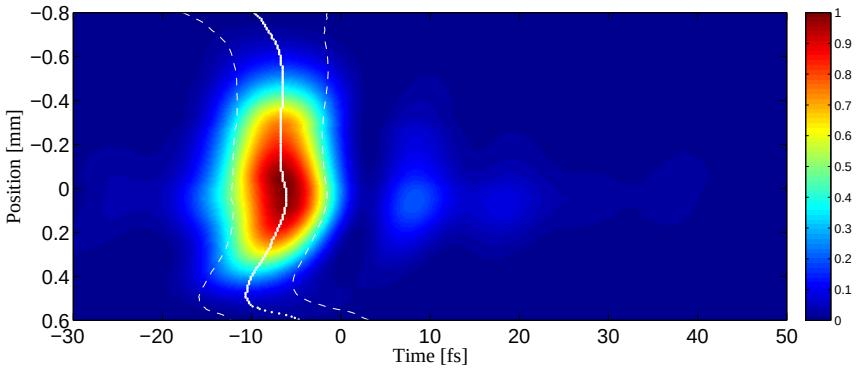

Fig. 5. Space-time temporal reconstruction of the test pulse with the first order (linear) pulse-front tilt removed. The spatially dependent time of arrival of the peak (dotted) and of the pulse and half-maximum intensities (dashed) are overlaid.

For our device, we performed spatial filtering of the ancillaries by passing through an adjustable aperture (iris). For small amounts of space-time coupling, as in our case, this is sufficient. We verified that this was sufficient filtering by monitoring for changes in the interferogram as a function of the iris diameter. More extensive spatial filtering could be performed, as described in [27], but at the expense of signal intensity. The spatial filtering ensures that the ancillary pulses have an approximately flat wavefront and frequency-independent propagation direction, thus acting as a constant reference across the spatial extent of the test pulse, enabling

#156765 - $15.00 USD Received 19 Oct 2011; revised 13 Nov 2011; accepted 14 Nov 2011; published 28 Nov 2011

the relative time-delays of each spatial slice to be measured. However, we did not perform an accurate calibration of the upconversion geometry, and therefore the first order (i.e. linear) pulse-front tilt cannot be measured. In order to measure small variations in the temporal intensity as a function of position, it is clear that accurate temporal measurements are key. We have therefore used the multiple shear method to ensure accurate temporal reconstructions for all spatial positions. A space-time temporal reconstruction is shown in Fig. 5 with the linear pulse-front tilt removed. Since the ancillary pulses were spatially filtered, higher order pulse-front tilt can be measured. The RMS deviation of the peak arrival time as a function of position was measured to be 0.68 fs (280 mrad, $\lambda_0 \sim 720$ nm). The spatial mean FWHM pulse duration is 10.2 fs with a RMS deviation of 0.4 fs. Thus it is evident that the space-time coupling output of the hollow fiber is minimal, and is thus an excellent source of few-cycle pulses for strong-field interactions such as high harmonic generation.

5. Conclusion

Intense pulses propagating in transparent media can result in a nonlinear interactions, significantly altering the temporal and spectral intensity and phase of the pulse. Such an effect can result in spectral broadening to over an octave, with very fine structure in both the intensity and phase (a signature of self-phase modulation), thus resulting in a large complexity / RMS time–bandwidth product, even though most of the pulse energy may be contained within a few femtoseconds. Due to the spectral broadening, only self-referencing methods are able to be used to completely characterize the temporal profile of the pulse. In the case of spectral-shearing interferometry, the choice of the shear used to measure the spectral phase is a key parameter of the measurement: it needs to be small enough to sample the fine structure adequately but also large enough to minimize noise accumulation across the spectrum and to step over any regions of low spectral intensity. For the correct choice of shear, it is possible to determine specific parameters of the pulse, such as GDD, pulse duration or peak power, with an accuracy better than 10% and with high precision (better than 0.5%). Using the multishear reconstruction, it was possible to verify the accuracy of the individual SPIDER phase measurements to be 0.1 rad (RMS). By combining multiple shear measurements, the precision and accuracy of the measurement process was significantly improved. This improved accuracy and precision enabled very precise quantification of the pulse time-bandwidth product and the space-time coupling in one transverse momentum (except for linear pulse-front tilt). Even though the pulse duration consisted of only several oscillations of the electric field over the pulse full width at half maximum, the TBP for the pulse was found to be quite large ($N_{50} = 125$) as a direct consequence of the structured spectral phase resulting from the nonlinear process. We also found minimal deviation in the pulse arrival time and pulse width (0.68 fs and 0.4 fs RMS respectively) as a function of a single transverse position in the beam. The benefits of spectral multishearing will be key in the study of strong field and relativistic experiments since accurate and precise measurements of the pulse are required to be able to perform accurate simulations of the experiments.

Acknowledgments

The authors acknowledge support from the Spanish Ministerio De Ciencia E Innovacion (MICINN) through its Consolider Program (SAUUL CSD 2007-00013), as well as through "Plan Nacional" (FIS2008-06368-C02-01) and the Catalan Agencia de Gestio dAjuts Universitaris i de Recerca (AGAUR) with SGR 2009-2013 Science and Humanities. I. A. W. and A. S. W. acknowledge support from the U.K. EPSRC (EP/H000178/1 and EP/F034601/1), the Leverhulme trust (F/08776/C) and the Royal Society. Funding from LASERLAB-EUROPE (228334) is gratefully acknowledged.

#156765 - $15.00 USD Received 19 Oct 2011; revised 13 Nov 2011; accepted 14 Nov 2011; published 28 Nov 2011